THE JOURNAL OF IMMUNOLOGY

B Cell Responses to a Peptide Epitope. V. Kinetic Regulation of Repertoire Discrimination and Antibody Optimization for Epitope

Bishnu P. Nayak, Renu Tuteja, Venkatasamy Manivel, Rajendra P. Roy, Ram A. Vishwakarma and Kanury V. S. Rao

J Immunol 1998;161;3510-3519

The Journal of Immunology is published twice each month by
The American Association of Immunologists, Inc.,
9650 Rockville Pike, Bethesda, MD 20814-3994.

Print ISSN: 0022-1767 Online ISSN: 1550-6606.

B Cell Responses to a Peptide Epitope. V. Kinetic Regulation of Repertoire Discrimination and Antibody Optimization for Epitope[1]

Bishnu P. Nayak,* Renu Tuteja,* Venkatasamy Manivel,* Rajendra P. Roy,† Ram A. Vishwakarma,† and Kanury V. S. Rao[2]*

The influence of imposing various conformational constraints on immune responses to a model epitope within a synthetic peptide immunogen was examined in mice. Although overall immunogenicity was affected, the model epitope (sequence DPAF) remained the predominant recognition site regardless of the conformation in which it was presented. A comparison of anti-DPAF mAbs obtained in response to two analogue peptides, PS1CT3 and CysCT3, in which the DPAF segment was either unconstrained or held within a cyclic loop, respectively, revealed a significant homology in the paratope composition. At one level a subset of anti-PS1CT3 and anti-CysCT3 mAbs was found to share a common heavy chain variable region. In addition, nucleotide sequence homology comparisons of both heavy and light chain variable regions identified the presence of anti-PS1CT3 and anti-CysCT3 mAbs that collectively appeared to derive from a common progenitor, but with nonidentical somatic mutations. Interestingly, however, no bias toward homologous Ag could be discerned on measurement of relative affinities of the mAbs for the two peptides. In contrast, mAb binding on-rates clearly discriminated between peptides representing the homologous vs the heterologous confomer of the DPAF epitope. Thus, it would appear that the kinetics of Ag recognition dominate over equilibrium binding criteria both in epitope-driven repertoire selection and Ab maturation in a humoral response. ***The Journal of Immunology*****, 1998, 161: 3510–3519.**

The antigenicity of domains on protein Ags has long been suspected to result from a variety of biophysical properties, such as backbone mobility, side chain stereochemistry, solvent accessibility, shape, secondary or three-dimensional structure, and local hydrophilicity (reviewed in Ref. 1). The underlying basis for such assumptions has been founded on the fact that B cells generally recognize protein Ags in their native form (1). Given that the preimmune B cell repertoire is not limiting (2), accessibility or easy availability for B cell recognition seemed to be the only intrusive criterion in identifying a B cell epitope. As a result, it was therefore logical to seek parameters that may help determine either surface exposure or ready accessibility of domains in a folded protein as direct correlates of antigenicity (3–8).

Recent results from our laboratory, however, have identified an additional constraint that intervenes to eventually determine the immunodominance of a given B cell epitope. We have shown that while the early primary T-dependent IgM response was indeed consistent with expectations, in that Abs were produced against all accessible domains, subsequent progression entailed stringent selection for only a restricted subset from the initially induced polyclonal pool (9). Positive selection of Ab specificities was found to be regulated by the ability of individual clonotypes to recruit the appropriate level of help, in a competitive environment, from a limiting pool of early Ag-activated Th cells (10). This, in turn, was dependent on both equilibrium (11, 12) and kinetic (13) binding properties of B cell surface Ig (sIg)[3] receptor recognition of its epitope on Ag, critical prognosticators that describe the Ag-presenting efficacy of a B cell. Thus, immunologic parameters implicated in modulating immunogenicity appear to prevail over determinants of antigenicity to eventually define the functional identity of putative B cell epitopes on polypeptide Ags.

The model antigenic determinant employed for the above studies was a 15-residue sequence (segment PS1) derived from the large envelope protein of hepatitis B surface Ag (HBsAg), in conjunction with one or more well-characterized T cell epitopes (12). We observed that the murine primary IgG response to such model immunogens was always directed exclusively against a tetrapeptide sequence (sequence: DPAF) encoded between positions 4 and 7 of the PS1 domain (10–13). The immunodominance of the DPAF sequence was independent of either the nature or the number of T cell epitopes included (10, 12). It was also independent of the position of the PS1 segment within the immunogen sequence (i.e., at the amino-terminal, middle, or carboxyl-terminal positions) (12). Finally, immunodominance of the DPAF epitope was also established in immunogen sequences of random structure, as determined by circular dichroism (CD) spectroscopy (12, 13), implying that accessibility for recognition was not the sole selection criterion. Such synthetic peptide antigens therefore represent good model systems to further understand both biophysical and immunologic parameters that help determine the immunodominance of a given B cell epitope.

Using analogues of a model peptide with different secondary structural propensities, we show here that immunodominance is independent of either perturbation in conformational preferences

*Immunology Group, International Center for Genetic Engineering and Biotechnology, and †National Institute of Immunology, Aruna Asaf Ali Marg, New Delhi, India

Received for publication January 5, 1998. Accepted for publication June 2, 1998.

The costs of publication of this article were defrayed in part by the payment of page charges. This article must therefore be hereby marked *advertisement* in accordance with 18 U.S.C. Section 1734 solely to indicate this fact.

[1] All nucleotide sequences described herein have been submitted to the EMBL database. Their accession numbers are from Y16445 to Y16464.

[2] Address correspondence and reprint requests to: Dr. Kanury V. S. Rao, Immunology Group, International Center for Genetic Engineering and Biotechnology, Aruna Asaf Ali Marg, New Delhi 110067, India.

[3] Abbreviations used in this paper: sIg, surface Ig; HBsAg, hepatitis B surface Ag; CD, circular dichroism; NMR, nuclear magnetic resonance; Aib, α-aminoisobutyric acid; TFE, trifluoroethanol; GC, germinal centers.

0022-1767/98/$02.00

or overall immunogenicity. Furthermore, both Ag-dependent repertoire discrimination and subsequent adaptation of Ab for optimal Ag binding appear to be regulated by the rapidity of binding rather than by the stability of it.

Materials and Methods

Materials

Horseradish peroxidase-labeled anti-mouse IgG (heavy chain specific) were purchased from Sigma (St. Louis, MO). F-moc amino acid derivatives were purchased from Novabiochem (Laufelfingen, Switzerland). For multipin synthesis of peptides, the noncleavable kits were obtained from Chiron Mimotopes (Victoria, Australia).

Peptide synthesis

Peptides were synthesized on a Milligen 9050 automated peptide synthesizer (Millipore, Bedford, MA) using F-moc chemistry (14–16). Crude peptides were purified to at least 95% purity by reverse phase HPLC on a C_{18} column (15 μm, δPak, 19 $\times$ 300 mm; Waters, Milford, MA). The identities of all peptides were ascertained by amino acid analysis.

For the synthesis of peptide CysCT3, the side chain protecting group used for cysteine was the acetamidomethyl group. Subsequent to synthesis and cleavage from the solid support, simultaneous deprotection of cysteine side chains and oxidation to form intramolecular disulfide bonds were achieved with iodine in acetic acid (17). Briefly, 70 mg of the acetamidomethyl-derivatized peptide was dissolved in 4 ml of 50% aqueous acetic acid. To this was added 1 ml of 1 M hydrochloric acid, followed immediately by 40 ml of a 50-mM solution of iodine in 50% aqueous acetic acid. After 30 min of vigorous stirring, the reaction was quenched with 2 ml of 1 M aqueous sodium thiosulfate. This was then concentrated in vacuo, following which it was passed over Celite. The resulting solution was lyophilized to yield the crude product, which was purified by reverse phase HPLC as described above. In addition to amino acid analysis, the correct identity of peptide CysCT3 could be established by mass spectrometry (expected mass, 3965; experimentally obtained mass, 3964.2).

Overlapping hexapeptide panels were synthesized by the method of Geysen (18) using the multipin noncleavable kits (Chiron Mimotopes, Victoria, Australia), strictly adhering to the protocol of the manufacturer. After completion of synthesis, all peptides were routinely acetylated at the amino terminus and subsequently deprotected as previously described (12).

Animals and immunizations

Female BALB/c mice (6–8 wk old) were obtained from the small animal facility at the National Institute of Nutrition (Hyderabad, India). Immunizations were given i.p. at a dose of 50 μg/mouse as an emulsion in CFA. For polyclonal sera, mice were bled from the retro-orbital plexus, and sera within a group were pooled.

Preparation of anti-CysCT3 IgG mAbs

A group of four BALB/c mice was immunized with a single dose of peptide CysCT3 as described above. Twenty-eight days later they were boosted with 50 μg/mouse of soluble peptide CysCT3 in PBS given i.v. Three days later, the highest responder from the group was taken for the generation of IgG-secreting hybridomas. Polyethylene glycol-mediated fusion to hypoxanthine-aminopterin-thymidine-sensitive myeloma derivative, SP2/O-Ag 14, maintenance of derived cell lines, and limiting dilution cloning were essentially as previously described (12, 19). The secretion of Ab in culture supernatants was screened by ELISA against wells coated with peptide CysCT3.

ELISAs

Plates were coated with 2 μg/well in 100 μl of PBS (pH 7.2) at 37°C for 3.5 h. Subsequently, they were blocked with 300 μl/well of a 5% solution of fat-free dry milk powder in PBS at 37°C for 1 h. Then, 100 μl of the appropriate dilution of mouse antiserum was added and incubated at 37°C for 1 h. After washing, bound Ab was detected with horseradish peroxidase-labeled secondary Ab (37°C, 1 h), followed by color development with *o*-phenylenediamine. Absorbance was measured at 490 nm.

For competitive ELISA experiments, antisera were used at dilutions representing 50% of the titer value. Twofold higher concentrations of antiserum and competitor peptide were mixed in equal volume and incubated for 10 min at room temperature. This was then added to duplicate wells at 100 μl/well. The remaining procedure was as described above.

ELISA assays for pin-bound peptides

The protocol for ELISA-based screening of Ab cross-reactivity with the overlapping hexapeptide panels has been described previously (12). Briefly, primary Abs were diluted to appropriate concentrations in PBS containing 2% BSA, 0.1% (v/v) Tween-20, and 0.1% (w/v) sodium azide. Pins were incubated in 200 μl each of Ab solution at 4°C overnight with gentle shaking. Subsequently, after washing they were then incubated with horseradish peroxidase-labeled goat anti-mouse IgG at room temperature for 1 h with gentle shaking. The chromogen used for revealing bound Ab was 2,2′-azino-bis-(3-ethylbenzthiazoline-6-sulfonic acid) diammonium, and absorbance was measured at 405 nm with subtraction of that at 490 nm.

Determination of on-rates and dissociation constants

On-rates of mAb binding to either peptide PS1CT3 or CysCT3 were determined as previously described (13). Briefly, equal volumes of mAb and appropriate peptide in PBS were mixed at room temperature, and time-dependent Ab binding in terms of quenching of tryptophan fluorescence was continuously monitored over a 100-min period in a Shimadzu RF-1501 spectrofluorometer (Shimadzu, Tokyo, Japan). The excitation wavelength used was 280 nm, and emission was recorded at 330 nm. The final Ab concentration employed was between 200 and 300 nM, whereas peptide was maintained at between 10- and 25-fold in molar excess over binding sites (assuming bivalency per Ab molecule) to ensure pseudo-first-order conditions. The extent of fluorescence quenching was used to determine unbound Ab concentrations as a function of time. The log of the concentration of unbound Ab was plotted vs time, and the slope, which was obtained by linear regression analysis, was used to determine k_{app}. The k_{on} value was subsequently calculated by dividing k_{app} by the peptide concentration. Values of k_{on} presented are the mean ($\pm$SD) of determinations at three independent peptide concentrations.

For dissociation constants, mAbs (final concentration between 100–150 μM) were incubated alone or with either peptide PS1CT3 or CysCT3 at concentrations ranging from 5×10^{-5} to 1×10^{-9} M at room temperature for 1 h. Subsequent to this extent of quenching of tryptophan, fluorescence was determined, from which the concentration of peptide bound was calculated assuming bivalency for each IgG molecule at saturation. K_d values were subsequently obtained from a Scatchard analysis of the resulting data.

Nuclear magnetic resonance (NMR) spectroscopy

Natural abundance, proton-decoupled (Waltz 16 decoupler) ^{13}C NMR spectra were recorded in a mixture of H_2O and D_2O (9:1) on a Brucker (Avance Series, DRS 300, Billerica, MA) spectrometer at 75.47 MHz. The spectral width was maintained at 19,607.84 Hz, with a time domain size of 65K. A total of 15,000 scans were accumulated at 300°K, using 3-(tetramethylsilyl)-1-propane sulfonic acid as the reference standard.

RT and amplification of IgG mRNA

Total cellular RNA was isolated from about 10^7 hybridoma cells with an RNAzol (Wak-Chemie Medical, Homburg, Germany)-based protocol with minor modifications. About 10 μg of total RNA was used for each V gene cDNA amplification. The first strand of cDNA was synthesized using 20 U of reverse transcriptase (Promega, Madison, WI) and 800 pmol of the primer, 5′-GGCCAGTGGATAGAC-3′ for Cγ and 5′-GCTCACTGGATGGTGGGAAGATG-3′ for Cκ, in a final volume of 25 μl. Single-stranded cDNA was then amplified using as 5′ primer, 5′-AGGT(C/G)(A/C)A(A/G)CTGCAG(G/C)AGTC(A/T)GG-3′ for V_H and 5′-GA(A/C/T)ATTGTG(A/C)T(G/C)AC(A/C)CA(A/G)(A/T)CTCCA-3′ for V_L. A different set of nested 3′ primers was used for amplification, 5′-GGCCAGTGGATAGAC(T/C/A)GA-3′ for Cγ and 5′- GAAGATGGATACAGTTGGTGCA-3′ for Cκ. Amplification was conducted using 5 μl of cDNA and Taq polymerase (Stratagene, La Jolla, CA) in a final volume of 100 μl. The final concentrations of reagents were 50 mM KCl, 10 mM Tris-HCl (pH 8.8), 1.5 mM $MgCl_2$, 0.01% gelatin, 200 pmol of each primer, and 2.5 U of Taq polymerase. PCR was performed on a Perkin-Elmer thermocycler using the following program: one cycle at 95°C for 3 min, followed by 30 cycles of 1 min each at 94°C, 58°C for 1.5 min, 72°C for 1 min, and finally a 10-min incubation at 72°C. A 10-μl aliquot of the reaction mixture was analyzed on a 1.8% agarose gel.

Nucleotide sequencing of the PCR-amplified DNA

PCR products of about 400 bp were blunt ended by polishing with the PCR polishing kit from Stratagene and were subsequently cloned in the *Srf*I site of PCR-script vector of the PCR-script cloning kit from Stratagene. Positive clones were identified, restriction digestion of plasmid DNA was performed, and appropriate clones were sequenced using the T7 sequencing kit purchased from Pharmacia (Uppsala, Sweden). Both strands of cloned

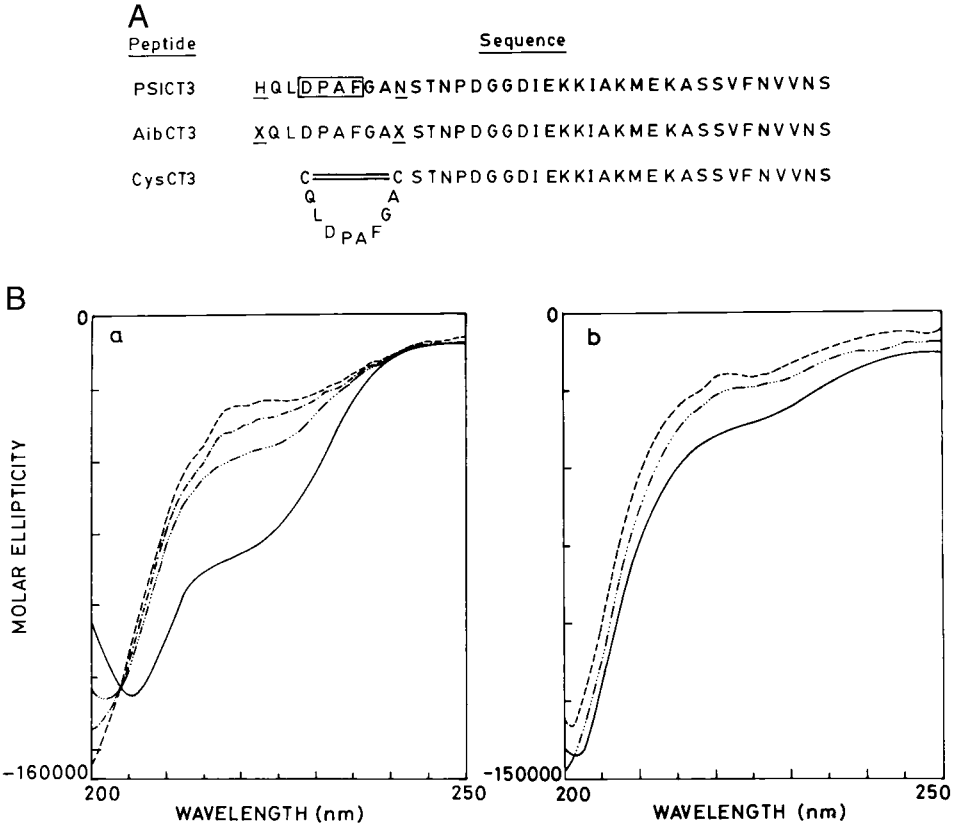

FIGURE 1. *A*, Amino acid sequence of peptide PS1CT3 and its analogues. The amino acid sequence of peptide PS1CT3 and its two analogues, peptides AibCT3 and CysCT3, are given here in the single letter code for amino acids. The His and Asn residues at positions 1 and 10 of the PS1CT3 sequence (underlined) have been replaced by Aib residues (indicated by the symbol X) in peptide AibCT3 and by Cys in peptide CysCT3. Residues 1 to 15 of the PS1CT3 peptide (segment PS1) correspond to a known B cell epitope of HBsAg, whereas residues 18 to 38 (segment CT3) constitute a promiscuous T cell epitope from the circumsporozoite protein of *P. falciparum* (12). Separating the B and T cell epitopes is a spacer of two glycine residues at positions 16 and 17. The immunodominant sequence, DPAF, in peptide PS1CT3 is highlighted within a box. The double bond between the Cys residues in peptide CysCT3 is meant to denote a disulfide bond. *B*, CD spectra of peptides Aib-PS1 (*a*) and PS1 (*b*) in aqueous and secondary structure-enhancing solvents. The CD spectra of peptide Aib-PS1 at a final concentration of 6 μM was recorded on a JASCO model J710 spectropolarimeter (JASCO, Tokyo, Japan) over a wavelength range of 200 to 250 nm with a step resolution of 0.1 nm and a scan speed of 200 nm/min. The spectra shown are those averaged over a total of 30 accumulations. *a* shows the CD spectra of peptide Aib-PS1 either in 0.01 M phosphate buffer (pH 7.2) alone (- - -) or in buffer containing 10% (- · -), 20% (- ··· -), or 50% (——) of TFE. *Panel b* shows the CD spectra obtained for a peptide representing the B cell epitope segment (residues 1–15) of the parent peptide PS1CT3 (peptide PS1) under identical conditions. This has been included for comparative purposes. In the latter case the profiles obtained in buffer alone and in the presence of 10% TFE were superimposable. As is evident, peptide Aib-PS1 shows a markedly greater helix-forming potential than peptide PS1. This is further supported by the occurrence of an isodichroic point in *panel a* at about 204 nm, which is indicative of TFE-dependent transition from random to a helical structure. No such isodichroic point is observed in the CD spectra of peptide PS1 (*b*).

DNA were sequenced. Normally two independent clones were sequenced for each mAb. However, in instances where any discrepancy was noted, additional clones were sequenced to rule out artifactual mutations as a result of the PCR procedure. The Ig heavy and light chain variable region gene sequences were analyzed using PC Gene software (Oxford Molecular Group PLC, Oxford, U.K.) and the GenBank data library.

Results

Peptide PS1CT3 and its analogues

The model parent immunogen (peptide PS1CT3; Fig. 1*A*) used in these studies has been described previously (10, 12, 14). Briefly, it represents a hybrid of a B cell epitope derived from the envelope protein of HBsAg (20) and a promiscuous T cell epitope resident within the circumsporozoite protein of the malaria parasite, *Plasmodium falciparum* (21). We have shown in prior studies that this peptide represents a T-dependent Ag and that immunization in BALB/c mice results in a primary and a secondary IgG response that is exclusively directed against a tetrapeptide sequence between positions 4 and 7 (sequence: DPAF) (12). Furthermore, based on a combination of results derived from an analysis of early primary IgM responses to peptide PS1CT3 and the CD spectrum of peptide, it was inferred that surface accessibility alone was an insufficient criterion to explain the immunodominance of the DPAF segment within peptide PS1CT3 (12).

To probe further whether altered conformational constraints of an epitope influences its immunodominance, we synthesized two additional analogues of peptide PS1CT3, namely, peptides AibCT3 and CysCT3 (Fig. 1*A*). Peptide AibCT3 represents an analogue where the amino acid residues at positions 1 and 10 in the parent sequence were substituted with α-aminoisobutyric acid (Aib), a nonnatural amino acid known to promote α-helix formation when introduced into peptide sequences (22). That Aib substitution also confers a propensity for helix formation in the present instance could be confirmed with the help of a synthetic peptide representing the B cell epitope segment (positions 1–15) of peptide AibCT3 (peptide Aib-PS1). Analysis of the CD spectra of this peptide in the presence of varying concentrations of the secondary structure-enhancing solvent, trifluoroethanol (TFE) (23), revealed ready inducibility into an α-helix (Fig. 1*B*, *a*). The second

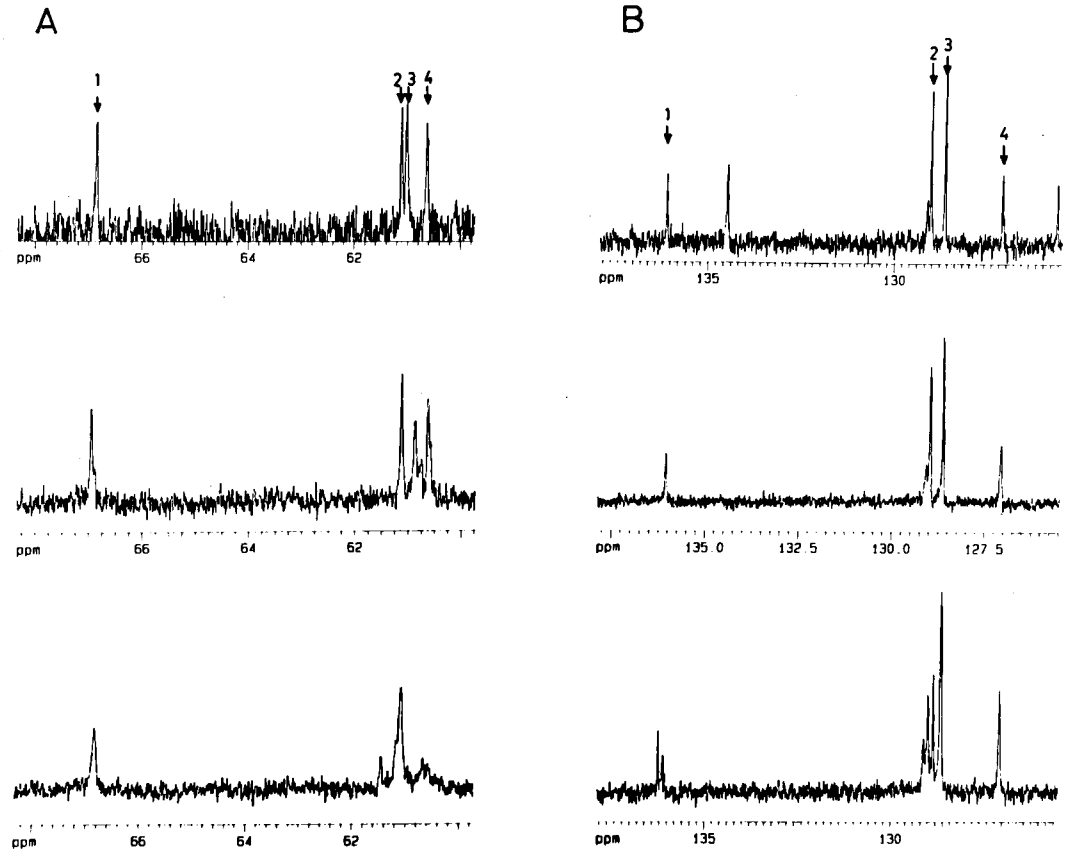

FIGURE 2. Proton-decoupled ^{13}C NMR spectra of peptides PS1, Aib-PS1, and Cys-PS1. For details refer to *Materials and Methods* and the text. Assignments of individual carbon atoms were performed with the help of published values for chemical shifts (53). Any ambiguity was resolved by obtaining spectra for the individual amino acids. The α-carbon atoms of the two proline residues at positions 5 and 14 were distinguished by heteronuclear multiple quantum coherence experiments. The identity of the extra signal at 61.4748 ppm for peptide Cys-PS1 in *A* remains presently unknown as does the reason for diffusion of the peak corresponding to the β-carbon of Thr^{12}.

analogue, peptide CysCT3, was one in which the residues at positions 1 and 10 were substituted with cysteines, subsequent to which this segment was locked into a loop by oxidation to generate a disulfide bond (Fig. 1*A*). Thus, while the immunodominant DPAF segment exists in a disordered conformation in peptide PS1CT3, it is conferred with an α-helical propensity in peptide AibCT3. In contrast, this segment was expected to be held within a relatively rigid cyclic loop in peptide CysCT3.

We were further able to verify that the substitutions performed do, in fact, variably influence conformational distributions of the DPAF epitope by NMR spectroscopy. While a detailed analysis will be published elsewhere (R. A. Vishwakarma, et al., manuscript in preparation), Figure 2 shows two relevant regions of proton-decoupled, natural abundance ^{13}C NMR spectra of peptides PS1, Aib-PS1, and Cys-PS1. Figure 2*A* represents that portion of the spectrum that includes the chemical shifts for the α-carbon atoms of proline residues. In peptide PS1 (*top panel*), the signal for the α-carbon of the proline residue at position 14 appears at 61.1314 ppm (peak 2), whereas that for the residue within the DPAF epitope (Pro^5) is further upfield at 61.0344 ppm (peak 3). Peaks 1 and 4 (66.9532 and 60.6537 ppm) correspond to the β- and α-carbons of the threonine residue at position 12 in the PS1 sequence. A comparison with the corresponding region of the spectrum for peptide Aib-PS1 (*middle panel*) reveals an interesting difference with respect to the α-carbon of the proline residue within the DPAF sequence (Pro^5). In the latter case an upfield shift to 60.8712 ppm was observed. Furthermore, this signal displayed multiplicity (Fig. 2*A*, *middle panel*), indicative of the existence of this carbon atom in a multiplicity of chemical environments, all of which were nonidentical with that for the corresponding carbon atom in peptide PS1. In contrast, the α-carbon of Pro^5 in peptide Cys-PS1 (Fig. 2*A*, *bottom panel*) was shifted downfield to merge with the signal for the α-carbon of Pro^{14}. While the signal for the α-carbon of Pro^5 was variably shifted depending upon either Aib or Cys substitution, the signals for the corresponding carbon atoms in Pro^{14} and Thr^{12} remained invariant among the three analogues (Fig. 2*A*).

Figure 2*B* gives the aromatic region of the ^{13}C NMR spectra of these peptides. The *top panel* is that for peptide PS1, where peak 1 represents the carbon at position 1 (with respect to β-carbon substitution) of the benzene ring of phenylalanine. Peaks 2 and 3 correspond to the ortho and meta aromatic carbons, respectively, whereas peak 4 represents the carbon in the para position. The remaining two signals are derived from the carbons in the imidazole ring of histidine, which are absent in peptides Aib-PS1 (*middle panel*) and Cys-PS1 (*bottom panel*). Although the distribution of signals for the aromatic carbons of Phe remain unchanged in the spectrum of peptide Aib-PS1, that for peptide Cys-PS1 reveals interesting differences (Fig. 2*B*, *bottom panel*). Signals for the aromatic carbons at both the 1 and ortho positions displayed multiplicity in the case of peptide Cys-PS1, indicative of differences in the chemical environment of the Phe residue in peptides PS1 and Cys-PS1.

Collectively, the data in Figure 2 clearly demonstrate that both Aib and Cys substitutions nonidentically perturb the stereochemical environment of the DPAF epitope with respect to that in peptide PS1.

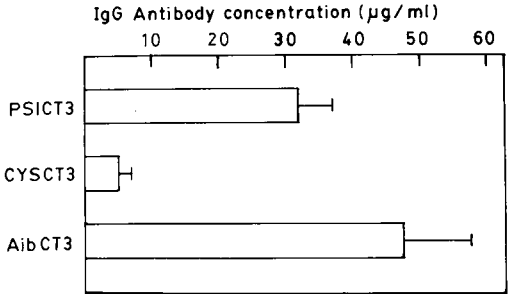

FIGURE 3. Relative immunogenicities of peptide PS1CT3 and its analogues. Groups of five BALB/c mice were immunized with peptide PS1CT3, AibCT3, or CysCT3 as emulsions in CFA (see *Materials and Methods*). Twenty-eight days later, the mice were bled, and peptide-specific serum IgG levels in pooled sera were quantitated by ELISA (see *Materials and Methods*). Values presented are the mean of three separate experiments from independent immunizations.

Relative immunogenicity of peptides PS1CT3, AibCT3, and CysCT3

Our initial studies were directed toward examining the effects of these modifications on the immunogenicity of the resulting peptides. For this, peptide PS1CT3 and its two analogues were independently immunized into groups of BALB/c mice, and the resulting specific IgG titers were monitored. As shown in Figure 3, secondary structure, or a preference for it, can influence immunogenicity. While Aib substitution resulted in a marginal enhancement of Ab titers, peptide CysCT3 was only weakly immunogenic (Fig. 3). More recent studies have indicated that the poor immunogenicity of peptide CysCT3 is a consequence of its poorer ability to prime Th cells (B. P. Nayak and K. V. S. Rao, unpublished observations).

Epitope specificity of the primary IgG response is independent of conformational constraints

We have shown earlier that the murine primary response to peptide PS1CT3 was exclusively directed against the B cell epitope segment (segment PS1) between positions 1 and 15, with no detectable Abs against the rest of the sequence (12). To confirm whether this was also true for peptides CysCT3 and AibCT3, we performed competitive inhibition ELISA experiments in which binding of day 28 IgG with either CysCT3 or AibCT3 was examined in the presence of either the homologous immunogen or a synthetic peptide representing only the homologous B cell epitope segment (residues 1–15) as inhibitor. The results from such an experiment are shown in Figure 4, where parallel data obtained for anti-PS1CT3 IgG is also included for comparison. Nearly identical inhibition profiles were obtained regardless of whether the whole homologous immunogen or only its derived B cell epitope segment was used as inhibitor, with virtually complete inhibition at higher concentrations. Further, a synthetic peptide representing the T cell epitope segment (residues 18–38) was also unable to inhibit Ab binding to any significant extent over the dose range tested in any of the cases (<10%; data not shown). Collectively, these results suggest that, similar to peptide PS1CT3, the specificity of primary IgG responses to peptides AibCT3 and CysCT3 is also at least predominantly restricted to within the amino-terminal 15 residues, with little or no response against the rest of the Ag sequences.

To further localize fine specificities, we resorted to epitope mapping with a panel of overlapping hexapeptides, displaced by one residue at a time, derived from the B cell epitope segment of each of these analogues. The results from such an experiment are shown in Figure 5. The cross-reactivity profile obtained with anti-PS1CT3 IgG is entirely consistent with our earlier observation, in that only three overlapping peptides (sequences: QLDPAF, LDPAFG, and DPAFGA) were recognized (12). This was shown to result from virtual monospecificity of the IgG response against a common tetrapeptide sequence, DPAF (12). Interestingly, almost identical results were obtained for both anti-AibCT3 and anti-CysCT3 IgGs (Fig. 5). Thus, although the modifications performed influenced immunogenicity, the fine specificity of the primary IgG response was apparently unaffected.

The monoclonal IgG response to peptide CysCT3 is predominantly monospecific but is genetically diverse

To distinguish between narrow range polyspecificity and monospecificity, we selected one analogue, peptide CysCT3, for further study. mAbs of the IgG class were generated using a protocol identical with that described for peptide PS1CT3 (12). A total of 13 mAbs were obtained, which were subsequently analyzed for cross-reactivity against the overlapping hexapeptide panel described in Figure 5. In addition, we determined the nucleotide sequence of the heavy chain variable regions of these mAbs. Results from both of these studies are summarized in Table I (mAbs Cys2 to Cys23).

Of the 13 mAbs obtained, 12 were directed exclusively against the DPAF sequence, whereas the remaining one, mAb Cys2, also

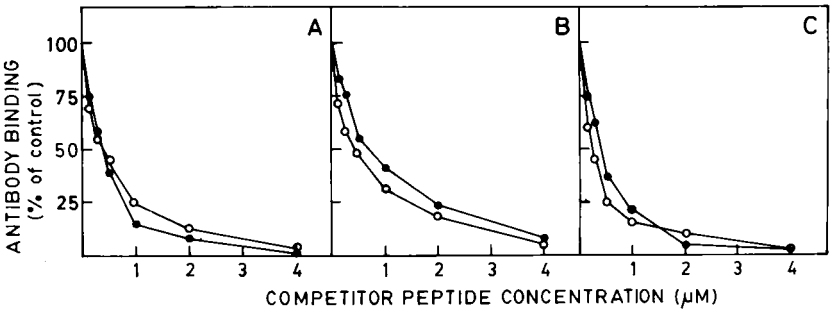

FIGURE 4. Anti-peptide polyclonal IgG responses are exclusively directed against the B epitope segment. Polyclonal day 28 antisera against peptide PS1CT3 (*A*), CysCT3 (*B*), or peptide AibCT3 (*C*) from Figure 2 were diluted to 50% of the titer value and incubated with the indicated final concentrations of either a peptide representing only the homologous B cell epitope (i.e., residues 1–15 of the peptide sequences depicted in Fig. 1*A*; ○) or the homologous immunogen (i.e., PS1CT3, CysCT3, or AibCT3; ●) as described in *Materials and Methods*. Subsequently, 100-μl aliquots were added in duplicate wells coated with homologous Ag, and bound Abs were determined by ELISA (see *Materials and Methods*). The results presented are a representative of three separate experiments.

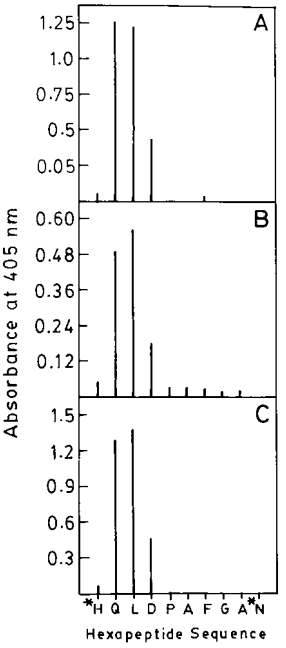

FIGURE 5. Monospecificity of the polyclonal day 28 IgG response to either peptide PS1CT3 or its analogues. Day 28 sera from Figure 2 obtained in response to peptide PS1CT3 (*A*), CysCT3 (*B*), or AibCT3 (*C*) were screened for IgG cross-reactivity against a panel of overlapping hexapeptides derived from the homologous B cell epitope segments of residues 1 to 15 (see Fig. 1*A*) as previously described (12). The *x*-axis denotes each hexapeptide as its N-terminal residue in the parent PS1 sequence. The stars on H and N indicate that these positions were substituted with either Cys (*B*) or Aib (*C*) when used to screen for anti-CysCT3 and anti-AibCT3 cross-reactivities. Results are presented as absorbance obtained for each hexapeptide after subtracting that obtained for a negative control peptide of sequence AQGNSM. This figure is a representative of three separate experiments. The serum dilutions used were 1/100 for anti-PS1CT3 and anti-AibCT3, and 1/50 for anti-CysCT3.

Table I. *Characterization of anti-CysCT3 and anti-PS1CT3 IgG mAbs*[a]

mAb	Heavy Chain V_H	Heavy Chain D_H	Heavy Chain J_H	CDR3 Sequence (amino acid)	Minimal Binding Sequence[b]
Cys-2	36–60	SP2.2	4	EGTSYAMDY	LDPAF
Cys-8	J558	SP2.4	3	WDGWLLLFAN	DPAF
Cys-18	J558	SP2.3	3	WAWFAY	DPAF
Cys-25	7183	SP2.2	3	PYDYDVAWFAY	DPAF
Cys–4	J558	FL16.2	4	GRATDYAMDY	DPAF
Cys-20	J558	FL16.2	4	GRATDYAMDY	DPAF
Cys-16	36–60	Q52	3	GGTGFAY	DPAF
Cys-24	36–60	Q52	3	GGTGFAY	DPAF
Cys-3	36–60	Q52	2	GGTGFDY	DPAF
Cys-7	36–60	Q52	2	GGTGFDY	DPAF
Cys-10	36–60	Q52	2	GGTGFDY	DPAF
Cys-11	36–60	Q52	2	GGTGFDY	DPAF
Cys-23	36–60	Q52	2	GGTGFDY	DPAF
PC2811	J558	FL16.1	2	FYY	DPAF
PC288	Misc.[c]	SP2.5	4	SGYYGNYVYAMDY	DPAF
PC2812	Misc.	SP2.5	4	SGYYGNYVYAMDY	DPAF
PC281	J558	Q52	2	AGNWDY	DPAF
PC282	J558	Q52	2	AGNWDY	DPAF
PC284	J558	Q52	2	AGNWDY	DPAF
PC285	J558	Q52	2	AGNWDY	DPAF
PC286	J558	Q52	2	AGNWDY	DPAF
PC287	36–60	Q52	2	GGTGFDY	DPAF
PC283	36–60	Q52	3	GGTGFTY	DPAF
PC289	36–60	Q52	3	GGTGFAY	DPAF

[a] Nucleotide sequences of the heavy chain variable region genes and identification of families to which individual segments belong were determined as previously described (9). The predicted amino acid sequence of the heavy chain CDR3 region is also given. Epitope fine specificities of individual mAbs were identified as described in the text. Gene segment families were identified either with the help of the GenBank database or by comparison with published sequences (54).

[b] Ab fine specificity data for the anti-PS1CT3 mAbs were taken from reference 12.

[c] The V_H genes of these mAbs could not be ascribed to any known family and therefore have been identified as miscellaneous (Misc.).

required the leucine residue at position 2 for optimal binding (Table I). Analysis of the nucleotide sequences of heavy chain variable regions revealed that these mAbs derive from no less than seven distinct precursor B cells (Table I). Interestingly, however, the genetic repertoire of these mAbs appeared to be biased, with as many as seven mAbs using V_H genes from the 36–60 family and a D_H Q52 gene (Table I). In addition, these seven mAbs shared a highly homologous heavy chain CDR3 region of consensus sequence GGTGFXY, where X denotes the sole position of variance in these regions (Table I).

We next determined the heavy chain nucleotide sequence of the anti-PS1CT3 mAbs described previously (12), the results of which are also summarized in Table I (mAbs PC2811 to PC 289). It is obvious that the monospecific anti-PS1CT3 IgG response similarly originates from an oligoclonal B cell population, with no less than four distinct B cell precursors contributing to it (Table I). Intriguingly, heavy chain variable regions of three of the 11 anti-PS1CT3 IgG mAbs (mAbs PC287, 283, and 289) bore a resemblance to the dominant anti-CysCT3 mAb population with V_H 36–60 and D_H Q52 usage, and a consensus CDR3 sequence of GGTGFXY (Table I). The substitution of Thr for Ala at position X in mAb 283 vis-a-vis mAb 289 represents a single nucleotide change in the corresponding codon. It is therefore likely that this change results from a point mutation as a consequence of somatic hypermutation during affinity maturation (24, 25).

The results presented in Table I reiterate that selective immunodominance of the DPAF epitope is retained regardless of whether it is presented within a linear segment or constrained within a disulfide-held loop. Further, there is a significant sharing of the Ab paratope phenotype repertoire between the corresponding mAb populations, at least at the level of the heavy chain variable region.

Affinity for Ag is not a criterion for repertoire distinction

The overlap in repertoires, at least at the level of the heavy chain, between anti-PS1CT3 and anti-CysCT3 IgG mAbs was intriguing. If one assumes that fusion is a purely stochastic process, then the frequency of occurrence of a particular Ab in an mAb panel is also likely to reflect the frequency of occurrence of the parent B cell in the Ag-activated B cell pool within the host. If this is true, then the data in Table I are indicative of a shift in the profile of dominant paratope phenotypes, at least at the level of the heavy chain, invoked by peptides PS1CT3 and CysCT3. Thus, while the heavy chains used by mAbs PC281, PC282, PC284, PC285, and PC286 constitute the dominant component of the anti-PS1CT3 mAb panel, it is the heavy chain used by mAbs PC283, PC287, and PC289 that predominates in the anti-CysCT3 mAb panel, being present in as many as seven of the 13 Abs (Table I). mAbs analogous to the remaining anti-PS1CT3 mAbs were not detected in the anti-CysCT3 panel, indicative either of a relatively lower frequency of occurrence or their absence from it.

Given the altered presentation of the DPAF segment by peptides PS1CT3 and CysCT3, we expected that the Ab repertoires induced by each of these Ags should discriminate between the homologous and heterologous Ags in terms of their binding properties. To assess this, we compared the relative affinities of anti-PS1CT3 and anti-CysCT3 mAbs for both homologous and heterologous Ags by

Table II. *Relative affinities of anti-PS1CT3 and anti-CysCT3 mAbs for homologous vs heterologous Ags*[a]

mAb	Inducing Ag	IC_{50} (μM) for Peptide	
		PS1CT3	CysCT3
PC288	PS1CT3	1.8 ± 0.5	2.6 ± 1.0
PC2812	PS1CT3	2.4 ± 0.3	2.8 ± 0.8
PC281	pS1CT3	3.3 ± 0.4	5.3 ± 1.7
PC282	PS1CT3	3.5 ± 0.3	4.2 ± 0.6
PC284	PS1CT3	3.1 ± 0.3	3.4 ± 0.2
PC285	PS1CT3	2.8 ± 0.8	3.6 ± 0.3
PC286	PS1CT3	2.6 ± 0.5	2.5 ± 0.1
PC287	PS1CT3	1.5 ± 0.3	1.2 ± 0.2
PC283	PS1CT3	1.4 ± 0.4	4.3 ± 0.2
PC289	PS1CT3	2.4 ± 0.3	4.8 ± 0.7
Cys2	CysCT3	1.3 ± 0.2	4.1 ± 0.6
Cys8	CysCT3	0.6 ± 0.2	2.4 ± 0.1
Cys18	CysCT3	1.6 ± 0.4	4.3 ± 0.5
Cys25	CysCT3	5.3 ± 0.2	3.9 ± 0.8
Cys4	CysCT3	2.0 ± 0.7	4.7 ± 0.4
Cys20	CysCT3	4.0 ± 1.0	6.2 ± 0.1
Cys16	CysCT3	1.6 ± 0.8	4.9 ± 1.0
Cys24	CysCT3	2.9 ± 0.6	3.0 ± 0.4
Cys3	CysCT3	1.3 ± 0.2	3.1 ± 0.5
Cys7	CysCT3	1.0 ± 0.3	2.8 ± 0.4
Cys10	CysCT3	1.6 ± 0.6	5.5 ± 0.4
Cys11	CysCT3	1.8 ± 0.5	5.4 ± 1.1
Cys23	CysCT3	1.0 ± 0.5	4.4 ± 0.5

[a] Relative affinities were estimated by competitive inhibition ELISA (*Materials and Methods*), and data are presented in terms of concentration of each peptide required to achieve 50% inhibition in Ab binding to surface-absorbed homologous Ag. Values are the mean (±SD) of three independent determinations.

competitive inhibition ELISA, and the results are given in Table II. It is evident that none of the mAbs displayed any significant difference in affinity for the homologous vs the heterologous peptide (Table II). This was equally true regardless of whether the mAbs were generated against peptide PS1CT3 or peptide CysCT3. Thus, affinity for Ag does not appear to constitute the discriminatory criterion for repertoire selection by peptide PS1CT3 vis-a-vis that by its homologue peptide CysCT3.

Clonal relatedness of anti-PS1CT3 and anti-CysCT3 mAbs employing a common Ig heavy chain

The anti-PS1CT3 and anti-CysCT3 mAbs bearing identical or near identical heavy chain CDR3 regions could be divided into two groups on the basis of heavy chain gene segment composition. The first group included mAbs PC283, PC289, Cys16, and Cys24, all of which use J_H3 in addition to a common D_H segment and an identical member of the 36–60 family of V_H genes (Table I). The only detectable difference represented replacement point mutations, which are likely to have arisen from somatic hypermutations in the course of the GC reaction (24–28). The second group, involving mAbs PC287, Cys3, Cys7, Cys10, Cys11, and Cys23 could be identified on the basis of utilization of the J_H2 gene segment with the remaining variable region gene segment composition being identical with that in group I (Table I). However, point mutational variations leading to amino acid replacements could again be observed among the mAbs of this group (Table I).

Given that both groups included representatives from the anti-PS1CT3 and anti-CysCT3 mAb panels, it was of interest to assess the degree of clonal relatedness between the members of each group. To this end we determined the nucleotide sequence of the mAb light chains after first establishing that all the mAbs in these two groups employed a light chain of the κ isotype. The salient features derived from such an analysis for the mAbs in both groups are summarized in Table III. With respect to group I, although mAbs PC283 and PC289 appear to employ a common light chain it was, nevertheless, distinct from that present in either mAb Cys16 or Cys24 (Table III). These distinctions were readily apparent at the level of both amino acid sequence of the CDR3 region and $J\kappa_L$ utilization (Table III). Thus, while it is possible that mAbs PC283 and PC289 represent mutational variants of a common precursor, it is clear that both mAb Cys16 and Cys24 derive from progenitors that are distinct from each other as well as from that for the anti-PS1CT3 subset. Nevertheless, given that all four mAbs in this group use Ig heavy chains with near homologous variable regions (Table I), at least some degree of structural homology may be expected at the level of paratope for all four mAbs in this group.

A comparison of light chain variable region nucleotide sequences of the group II subset of mAbs revealed that in addition to sharing derivatives of a common heavy chain variable region, all these mAbs bore light chains with, barring a few point mutations, identical variable regions (Table III). The near negligent probability of B cells deriving from independent lineages sharing a common gene segment composition for variable regions of both heavy and light chains with identical CDR3 regions (29) strongly suggests that mAbs PC287 and the anti-CysCT3 subsets in this group represent progenitors derived from a common precursor.

Ag discrimination by the anti-CysCT3 and anti-PS1CT3 mAbs is characterized by differences in the kinetics of recognition

The mAbs described in group I presented an interesting case of distinct but, nonetheless, structurally homologous anti-DPAF Ab paratopes independently induced by nonidentical presentation of the DPAF epitope by peptides PS1CT3 and CysCT3. On the other

Table III. *Light chain variable region composition of anti-PS1CT3 and anti-CysCT3 mAbs in groups I and II*[a]

Group	mAb	Inducing Ag	Light Chain (κ)		Amino Acid Sequence of:		
			V_L	J_L	CDR1	CDR2	CDR3
I	PC283	PS1CT3	5	1	KASENVGTYVS	GASNRYT	GQTYSYP
	PC289	PS1CT3	5	1	KASENVGTYVS	GASNRYT	GQTYSYP
	Cys16	CysCT3	5	5	KASENVGTYVS	GASNRYT	GQSYSHPL
	Cys24	CysCT3	3	2	RASKSVSTSGYSYMH	LVSNLES	QHIRELT
II	PC287	PS1CT3	5	5	KASENVDTYVS	GASNRYT	GQSYSYPL
	Cys3	CysCT3	5	5	KASENVGTYVS	GASNRYT	GQSYSYPP
	Cys7	CysCT3	5	5	KASENVGTYVS	GASNRYT	GQSYSYPP
	Cys10	CysCT3	5	5	KASENVGTYVS	GASNRYT	GQSYSYPP
	Cys11	CysCT3	5	5	KASENVGTYVS	GASNRYT	GQSYSYPP

[a] Deduced amino acid sequence of the CDR regions of the light chains utilized by the mAbs in groups I and II are given. These were derived from nucleotide sequencing of the light chain variable region genes as described in *Materials and Methods*.

Table IV. *Selectivity for the homologous Ag by both group I and II mAbs is evidenced at the level of Ag-binding kinetics*[a]

Group	mAb	Inducing Ag	K_d (M) $\times 10^{-8}$ for Peptide		k_{on} ($1.m^{-1}s^{-1}$) $\times 10^5$ for Peptide	
			PS1CT3	CysCT3	PS1CT3	CysCT3
I	PC283	PS1CT3	2.0 ± 0.6	1.4 ± 0.8	1.0 ± 0.32	0.13 ± 0.06
	PC189	PS1CT3	5.1 ± 1.2	4.8 ± 1.7	2.3 ± 0.51	0.10 ± 0.04
	Cys16	CysCT3	3.1 ± 0.7	2.8 ± 0.6	0.60 ± 0.23	5.10 ± 0.62
	Cys24	CysCT3	3.8 ± 0.7	3.3 ± 0.7	0.07 ± 0.03	1.15 ± 0.35
II	PC287	PS1CT3	1.8 ± 0.9	1.5 ± 0.6	5.60 ± 0.50	0.09 ± 0.03
	Cys3	CysCT3	3.2 ± 1.2	3.6 ± 0.8	1.24 ± 0.35	20.00 ± 3.20
	Cys7	CysCT3	1.6 ± 0.4	1.9 ± 0.6	2.80 ± 0.42	43.00 ± 6.40
	Cys10	CysCT3	2.8 ± 1.6	2.1 ± 0.9	2.40 ± 0.83	51.00 ± 5.30
	Cys11	CysCT3	3.8 ± 1.4	2.7 ± 1.1	2.90 ± 0.76	49.40 ± 5.50
	Cys23	CysCT3	2.4 ± 0.4	2.6 ± 0.5	0.10 ± 0.04	1.45 ± 0.24

[a] Determination of on-rate binding constants (k_{on}) and data presentation are as described in *Materials and Methods*. Values are the mean (±SD) of determinations at three separate peptide concentrations. Dissociation constants (K_d) were also obtained as described in *Materials and Methods*, and values are the mean (±SD) of three independent determinations.

hand, the anti-PS1CT3 and anti-CysCT3 mAbs in group II represent diversified progeny derived from a single precursor. The occurrence of nonidentical replacement mutations in the variable regions of the anti-PS1CT3 vs anti-CysCT3 mAbs suggested that at least some degree of differential optimization for the variably presented epitope had indeed taken place. Of particular interest were two distinctive substitutions that could be noted in the light chain CDR sequences of these mAbs. The first was the occurrence of the Asp residue at position 7 of CDR1 in mAb PC287, as opposed to Gly in the anti-CysCT3 mAbs, and the second was a Leu to Pro change at position 8 of the CDR3 region (Table III). It is likely that these distinctive substitutions may have been specified by the confomer of the DPAF epitope against which the respective mAbs were generated. Consequently, it was surprising that none of the mAbs in either group displayed a preference for the homologous Ag in terms of binding affinity, at least when measured as IC_{50} values (Table II).

To further probe for differences in Ag selectivity, we next determined the on-rates of binding of either peptide PS1CT3 or peptide CysCT3 to the mAbs in both groups by tryptophan fluorescence quenching assays. In addition, to eliminate any potential ambiguities, we estimated the equilibrium dissociation constants for these interactions using the same technique. The cumulative data from these experiments are given in Table IV. Although K_d values for mAb binding to the homologous vs heterologous Ag were similar, there was a distinct bias in favor of the homologous peptide when binding on-rates were compared (Table IV). This was equally true of mAbs in both groups. Thus, in group I, while the anti-PS1CT3 mAbs PC283 and PC289 bound the homologous peptide with on-rates that were markedly higher than that for peptide CysCT3. the reverse was true for the anti-CysCT3 mAbs, Cys16 and Cys24 (Table IV). Similarly, in group II, all anti-CysCT3 mAbs consistently bound the homologous peptide with on-rates that were between 14- to 21-fold higher than that for peptide PS1CT3 (Table IV). On the other hand, despite the comparable K_d values, mAb PC287 bound peptide PS1CT3 with an on-rate that was 62-fold higher than that for peptide CysCT3 (Table IV).

The mAb panels described in groups I and II permit two distinct levels of analysis. The group I mAbs represent altered repertoire recruitment as a consequence of presentation of the DPAF epitope in either a linear or a cyclic segment. On the other hand, the group II mAbs represent B cell derivatives of a common progenitor, but with divergent adaptation to the context of DPAF presentation either within a linear or a cyclic segment. Thus, the data in Table IV strongly suggest that kinetic, rather than equilibrium, binding parameters predominate in defining both Ab repertoire recognition of an epitope and subsequent maturation in a humoral response.

Discussion

Although surface accessibility is undoubtedly a prerequisite, recent results (9–13) now suggest that downstream, immune-mediated mechanisms will also need to be taken into consideration to explain the hierarchical immunodominance of B cell epitopes on protein Ags (30–38). An intriguing observation pertaining to this issue was our findings on the immunodominance of the DPAF sequence in segment PS1 when placed in the context of a variety of alternate sequences (9, 12). This was found to be independent of the position of the PS1 sequence in the Ag, the nature of the flanking domains, and also the genetic background of the mouse strain employed (9–13). Indeed, regardless of the influence of such changes on the overall immunogenicity of the resulting molecules, thereby implying quantitative differences in B cell recognition, the DPAF segment was always the most immunodominant among the various epitopes presented by the Ag (12). Having previously ruled out a role for position within the immunogen or nature of flanking sequence (9, 12), in the present study we sought to explore how perturbations in the conformational degrees of freedom of the segment encoding the DPAF epitope would influence its immunodominance relative to the rest of the molecule.

An alteration in the degrees of freedom of the amino-terminal 10-residue segment was alternatively achieved by substitution at appropriate positions with Aib residues to confer a bias toward α-helix formation or with cysteine residues to enable subsequent cyclization. That such substitutions indeed influenced the local environment within the DPAF epitope could be verified by an analysis of the ^{13}C NMR spectra of these peptides. An effect on the immunogenicity of the alterations performed was also observed on immunization of mice with the resultant analogues. While peptide AibCT3 yielded primary IgG Abs that were marginally higher than those against the parent peptide PS1CT3, those against peptide CysCT3 were markedly diminished. Surprisingly, however, this effect on immunogenicity did not translate into altered profiles of relative immunodominance among the putative epitopes contained within these Ags. The apparent monospecificity of the anti-CysCT3 response could be further verified by generating mAbs, all of which were found to be confined to recognition of the DPAF sequence. Thus, in addition to factors described earlier, the relative

immunodominance of the DPAF epitope is also insensitive to perturbations in the conformational degrees of freedom available to the segment within which it is contained. Furthermore, the observations reported here and previously (12) that preponderance of the anti-DPAF Ab population was independent of overall immunogenicity strongly imply that parameters involved in defining immunogenicity of a multideterminant Ag are independent of those that influence interepitopic hierarchy on the same Ag.

The analogues described here also provided us with an opportunity to examine how variations in the conformational freedom of an epitope qualitatively influence repertoire selection and maturation from the preimmune B cell pool. This was possible since all three peptides produced, almost exclusively, an anti-DPAF response. For this purpose we selected only one of the analogues, peptide CysCT3, as it was expected that a covalent disulfide-mediated ring closure would enforce a greater degree of rigidity as opposed to Aib substitution. A comparison of the anti-PS1CT3 and anti-CysCT3 mAb panels revealed that an alteration in the conformational propensities of the DPAF epitope did not lead to complete repertoire diversification. Rather, a partial overlap between the two sets was observed on comparison of the Ig heavy chain variable regions. This suggests at least some degree of similarity between the independently derived paratope phenotypes. Although both the anti-PS1CT3 and anti-CysCT3 mAb panels also included distinct members, the stochastic nature of the fusion process does not permit an inference as to whether they represent unique Ag-specific products or simply reflect differences in clonal population sizes in in vivo responses to the two Ags.

Considering the fact that peptides PS1CT3 and CysCT3 represent confomer variants of the same epitope, we had anticipated that the anti-PS1CT3 and anti-CysCT3 mAbs would display selectivity in terms of binding behavior for the homologous vis-a-vis heterologous confomer. Surprisingly, this did not hold true on comparison of the relative affinities for the two Ags. No significant differences in relative affinity could be detected for the two peptides with any of the mAbs tested. To investigate further we next selected those anti-PS1CT3 and anti-CysCT3 mAb subsets that shared a common heavy chain variable region, after accounting for point mutations as possible derivatives of the somatic hypermutation pathway in GCs. The underlying rationale for such a selection was based on the premise that a comparison between homologous paratope phenotypes would serve as a more reliable and accurate indicator of nuances in Ag selectivity if any. Such mAbs could subsequently be segregated into two groups based on the utilization of either the J_H3 (group I) or the J_H2 (group II) gene segment. By nucleotide sequencing of the light chain variable regions of mAbs in group I we were able to establish the independent clonal origins of the two anti-CysCT3 mAbs as well as their nonidentity with the anti-PS1CT3 mAbs of this group. In contrast, at least based on gene segment composition and CDR3 regions of both heavy and light chain variable regions, the mAb panel described in group II appeared to share a common precursor. Thus, the mAbs representing both groups seemed to us to provide two levels at which Ag-driven repertoire discrimination could be examined. Based on the commonality of the heavy chain variable region but the diversity in that of the light chain, the anti-PS1CT3 and anti-CysCT3 mAbs in group I could be considered as a case of a relatively minor Ab paratope repertoire shift in response to the different DPAF confomer variants. On the other hand, the group II mAbs represented an interesting example of a single precursor Ab that had divergently adapted to optimally accommodate the variant epitope confomers presented by peptides PS1CT3 and CysCT3. The presence of nonidentical replacement mutations in the paratope components of the anti-PS1CT3 vs anti-CysCT3 mAbs strongly suggested that some degree of Ag-specific adaptation had indeed occurred.

In contrast to the lack of discrimination at the level of affinities, the facility of epitope recognition, as indicated by binding on-rates, was found to correlate well with the Ag that was used to elicit a particular mAb of either group. Thus, for example in group I, mAbs PC283 and PC289 bound the homologous peptide PS1CT3 with on-rates that were 8- to 23-fold higher than that for the heterologous peptide CysCT3. On the other hand, the reverse was true for mAbs Cys16 and Cys24 where the rate of peptide CysCT3 binding was much higher than that for peptide PS1CT3. Similarly, a pronounced bias in favor of the homologous confomer, in terms of binding on-rates, was also noted for the anti-PS1CT3 and anti-CysCT3 counterparts assigned to group II. This consistent observation for groups I and II that Ag specificity correlates with the kinetics of epitope recognition but not with the affinity of it strongly suggests that both Ag-specified discrimination between Ab repertoires and Ab optimization for epitope binding, by way of somatic mutations and subsequent positive selection in GCs, are under kinetic control. Our latter inference is entirely consistent with prior studies by Foote and Milstein (39), who have already demonstrated that intraclonal selection of mutated B lymphocytes in GCs is kinetically driven. Nevertheless, our results provide an added perspective in also suggesting that improvement of an Ab-epitope fit in GCs may primarily represent a kinetic optimization.

While the high affinity of anti-PS1CT3 and anti-CysCT3 mAbs obtained in the early stages of a humoral response is surprising, it is consistent with more recent findings in other systems. Thus, for example, Zinkernagel and co-workers have shown that murine primary responses to vesicular stomatitis virus is composed of very high affinity Abs (40). More recently, Smith et al. (41) have demonstrated the presence of high affinity Ab-forming cells in primary humoral responses to the hapten (4-hydroxy-3-nitrophenyl)acetyl. Collectively, these studies suggest that optimal affinities for Ag may be achieved early, perhaps even before recruitment of B cells within germinal centers (GCs) (40, 41). Under such conditions, therefore, it may be expected that further optimization of Ag-Ab binding may be restricted to kinetic considerations.

Although our findings that optimization of the paratope-epitope fit is regulated by the kinetics of the interaction may appear to deviate from the common assumption that affinity for Ag plays the pivotal role (42–46), it is, however, consistent with our current understanding of the induction and progression of primary T-dependent humoral responses. It is now generally accepted that an Ag-activated B cell is constantly faced with the opposing choices of either positive selection for survival or death (47), the deciding factor being the ability of such B cells to recruit T cell help (10). Thus, in a competitive environment, such as that presented by GCs (24–28), where the available pool size of Th cells is limiting, rapid recruitment of T help by a given B cell is likely to confer on it an advantage for survival over alternate, competing clonotypes. Indeed, our own recent results have demonstrated that the quantum of T cell help recruited by an Ag-activated B cell is proportional to the on-rate of Ag binding to its sIg receptor (13). This presumably relates to the rate at which such B cells can generate a high enough ligand density on the cell surface to ensure TCR triggering above the requisite threshold value (48, 49). Consequently, it is perhaps not surprising that those clonal variants in GCs kinetically optimized for epitope binding are the ones that are selected.

The revelation that Ab optimization for epitope conformation is kinetically determined would also imply that facility of an epitope fit assumes premium over the perfection of such a fit. This may explain the high frequency of occurrence of flexible domains on protein Ags as B cell epitopes (7, 50). Further, this observation

may serve to rationalize the anomalous findings of imperfect Ag-Ab interfaces in the x-ray crystal structure of a variety of immune complexes (51, 52).

In summary, the results presented here provide evidence to support the following inferences. 1) Relative immunodominance of a peptidic B cell epitope is independent of the conformational constraints imposed on it. We stress here again that our interpretation limits to varying degrees of conformational freedom as opposed to transitions from one discrete secondary structural form to another. 2) Kinetics override equilibrium binding criteria in mediating Ag-specified discrimination between alternate possible Ab repertoire subsets. 3) Positive selection following somatic hypermutation in GCs is biased in favor of a kinetic optimum. Finally, our studies reported here also highlight the utility of appropriately designed model peptide Ags as novel probes to delineate mechanisms regulating humoral responses.

Acknowledgments

We thank Mr. B. Ganesan for amino acid and mass spectrometric analysis of the peptides. We also thank Dr. Dinakar Salunke (National Institute of Immunology, New Delhi, India) for many helpful discussions. We acknowledge many useful suggestions from the referees.

References

1. Colman, P. M. 1988. Structure of antibody-antigen complexes: implications for immune recognition. *Adv. Immunol. 43:99.*
2. Paige, C. J., and G. E. Wu. 1989. The B cell repertoire. *FASEB J. 3:818.*
3. Benjamini, C. J., J. A. Berzofsky, I. J. East, F. N. Gurd, C. Hannum, S. J. Lach, E. Margolies, J. G. Michael, A. Miller, E. M. Prager, M. Reichlin, E. E. Sercarz, S. J. Smith-Gill, P. E. Todd, and A. C. Wilson. 1984. The antigenic structure of proteins: a reappraisal. *Annu. Rev. Immunol. 2:67.*
4. Berzofsky, J. A. 1985. Intrinsic and extrinsic factors in protein antigen structure. *Science 229:932.*
5. Novotny, J., M. Handschumacher, E. Haber, R. E. Bruccoleri, W. B. Carlson, D. W. Fanning, J. A. Smith, and G. D. Rose. 1986. Antigenic determinants in proteins coincide with surface regions accessible to large probes (antibody domains). *Proc. Natl. Acad. Sci. USA 83:226.*
6. Thornton, J. M., M. S. Edwards, W. R. Taylor, and D. J. Barlow. 1986. Location of 'continuous' antigenic determinants in the protruding regions of proteins. *EMBO J. 5:409.*
7. Novotny, J., M. Handschumacher, and R. E. Bruccoleri. 1987. Protein antigenicity: a static surface property. *Immunol. Today 8:26.*
8. Geysen, H. M., J. A. Tainer, S. J. Rodda, T. J. Mason, H. Alexander, E. D. Getzoff, and R. A. Lerner. 1987. Chemistry of antibody binding to a protein. *Science 235:1184.*
9. Tuteja, R., A. Agarwal, L. Vijayakrishnan, B. P. Nayak, S. K. Gupta, V. Kumar, and K. V. S. Rao. 1997. B cell responses to a peptide epitope. II. Multiple levels of selection during maturation of primary responses. *Immunol. Cell. Biol. 75:245.*
10. Agarwal, A., and K. V. S. Rao. 1997. B cell responses to a peptide epitope. III. Differential T helper cell thresholds in recruitment of B cell fine specificities. *J. Immunol. 159:1077.*
11. Vijayakrishnan, L., V. Kumar, J. N. Agrewala, G. C. Mishra, and K. V. S. Rao. 1994. Antigen-specific early primary humoral responses modulate immunodominance of B cell epitopes. *J. Immunol. 153:1613.*
12. Agarwal, S., S. Sarkar, C. Nazabal, G. Balasundaram, and K. V. S. Rao. 1996. B cell responses to a peptide epitope. I. The cellular basis of restricted recognition. *J. Immunol. 157:2779.*
13. Vijayakrishnan, L., S. Sarkar, R. P. Roy, and K. V. S. Rao. 1997. B cell responses to a peptide epitope. IV. Subtle changes in flanking residues modulate immunogenicity. *J. Immunol. 159:1809.*
14. Merrifield, R. B. 1986. Solid phase synthesis. *Science 232:341.*
15. Stewart, J. M., and J. D. Young. 1984. *Solid Phase Peptide Synthesis*, 2nd Ed. Pierce Chemical Co., Rockford, IL.
16. Atherton, E., and R. C. Sheppard. 1989. *Solid Phase Peptide Synthesis: A Practical Approach.* IRL Press, Oxford, U.K.
17. Wade, J. D., S. P. Fitzgerald, M. R. McDonald, J. G. McDouggal, and G. W. Tregear. 1986. Solid phase synthesis of α-human atrial natriuretic factor: comparison of the Boc-polystyrene and Fmoc-polyamide methods. *Biopolymers 25:521.*
18. Geysen, H. M., S. J. Rodda, T. J. Mason, G. Tribbick, and P. G. Schoofs. 1987. Strategies for epitope analysis using peptide synthesis. *J. Immunol. Methods 102:259.*
19. Coligon, J. E., A. M. Kruisbeck, D. M. Margolies, E. M. Shevach, and W. M. Stoker. 1991. *Current Protocols in Immunology*. John Wiley & Sons, New York, p. 25.
20. Neurath, A. R., and S. B. H. Kent. 1988. The pre-S region of hepadna virus envelope protein. *Adv. Virus Res. 34:64.*
21. Sinigaglia, F., M. Guttinger, J. Kilgus, D. M. Doran, H. Matile, H. Etlinger, A. Trezciak, D. Gillessen, and J. R. K. Pink. 1988. A malaria T cell epitope recognized in association with most mouse and human MHC class II molecules. *Nature 336:778.*
22. Balaram, P. 1992. Non-standard amino acids in peptide design and protein engineering. *Curr. Opin. Struct. Biol. 2:845.*
23. Sonnichsen, F. D., J. R. Van Eyk, R. S. Hodges, and B. D. Sykes. 1992. Effect of trifluoromethanol in protein secondary structure: an NMR and CD study using a synthetic actin peptide. *Biochemistry 31:8790.*
24. Neuberger, M. S., and C. Milstein. 1995. Somatic hypermutation. *Curr. Opin. Immunol. 7:267.*
25. Kelsoe, G. 1995. In situ studies of the germinal center reaction. *Adv. Immunol. 60:267.*
26. Leanderson, T., E. Kallberg, and D. Gray. 1992. Expansion, selection and mutation of antigen-specific B cells in germinal centers. *Immunol. Rev. 126:47.*
27. Nossal, G. J. V. 1994. Differentiation of the secondary B lymphocyte repertoire: the germinal center reaction. *Immunol. Rev. 137:173.*
28. Kelsoe, G. 1995. The germinal center reaction. *Immunol. Today 16:324.*
29. Litwin, S., and M. Schlomchik. 1990. A test for clonal relatedness in a set of lymphocytes. *J. Exp. Med. 171:293.*
30. Bona, C. A. 1992. Expression of V gene families during ontogeny and establishment of the B cell repertoire. *Int. Rev. Immunol. 8:83.*
31. Wicker, L. S., C. D. Benjamini, A. Miller, and E. E. Sercarz. 1984. Immunodominant protein epitopes. II. The primary antibody response to hen egg white lysozyme requires and focuses upon a unique N-terminal epitope. *Eur. J. Immunol. 14:447.*
32. Scheerlinck, J. Y., R. De Leys, E. Saman, L. Brys, A. Geldhoff, and P. D. Bactselier. 1993. Redistribution of a murine humoral response following removal of an immunodominant B cell epitope from a recombinant fusion protein. *Mol. Immunol. 30:733.*
33. Berzofsky, J. A., L. K. Richman, and D. J. Killion. 1979. Distinct H-2 linked Ir genes control both antibody and T cell responses to different determinants on the same antigen, myoglobin. *Proc. Natl. Acad. Sci. USA 76:4606.*
34. Kunkl, A., D. Fenogglio, F. Manca, G. L. Pira, C. Cambiaggi, R. Strom, and F. Celada. 1992. Kinetic immunodominance: functionally competing antibodies against exposed and cryptic epitopes of *Escherichia coli* B-galactosidase are produced in time sequence. *Int. Immunol. 4:627.*
35. Manca, F., D. Fenoglio, A. Kunkl, C. Cambiaggi, L. Pira, and F. Celada. 1988. B cells on the podium: regulatory roles of surface and secreted immunoglobulin. *Immunol. Today 143:15.*
36. Herzenberg, L. A., and T. Tokushita. 1982. Epitope-specific regulation. I. Carrier induced suppression for IgG anti-hapten antibody response. *J. Exp. Med. 155: 1730.*
37. Sadegh-Nasseri, S., D. E. Knipp, B. A. Taylor, A. Miller, and E. E. Sercarz. 1984. Selective reversal of H-2 linked genetic unresponsiveness to lysozyme. I. Non-H-2 gene(s) closely linked to the Ir-2 locus on chromosome 2 permit(s) an anti-lysozyme response in H-2^b mice. *Immunogenetics 20:535.*
38. Sadegh-Nasseri, S., V. Dessi, and E. E. Sercarz. 1986. Selective reversal of H-2 linked genetic unresponsiveness to lysozyme. II. Alterations in T helper/T suppressor balance owing to gene(s) linked to Ir-2 leads to responsiveness in BALB/c mice. *Eur. J. Immunol. 16:486.*
39. Foote, J., and C. Milstein. 1991. Kinetic maturation of an immune response. *Nature 352:530.*
40. Roost, H.-P., M. F. Bachmann, A. Haag, U. Karlinke, V. Pliska, H. Hengartner, and R. M. Zinkernagel. 1995. Early high-affinity neutralizing anti-virus IgG responses without further overall improvement of affinity. *Proc. Natl. Acad. Sci. USA 92:1257.*
41. Smith, K. G. C., A. Light, G. J. V. Nossal, and D. M. Tarlinton. 1997. The extent of affinity maturation differs between the memory and antibody-forming cell compartments in the primary immune response. *EMBO J. 16:2996.*
42. Nossal, G. J. V. 1992. The molecular and cellular basis of affinity maturation in the antibody response. *Cell 68:1.*
43. Berek, C., and M. Zeigner. 1993. The maturation of the immune response. *Immunol. Today 14:400.*
44. Zeigner, M., G. Steinhauser, and C. Berek. 1994. Development of antibody in single germinal centers: selective expansion of high affinity variants. *Eur. J. Immunol. 24:2393.*
45. Kelsoe, G. 1996. The germinal center reaction: a crucible for lymphocyte selection. *Immunology 8:179.*
46. Rajewsky, K. 1996. Clonal selection and learning in the antibody system. *Nature 381:751.*
47. Kelsoe, G. 1996. Life and death in germinal centers. *Immunity 4:107.*
48. Valitutti, S., S. Muller, M. Cella, E. Padovan, and A. Lanzavecchia. 1995. Serial triggering of many T cell receptors by a few peptide-MHC complexes. *Nature 375:148.*
49. Viola, A., and A. Lanzavecchia. 1996. T cell activation determined by T cell receptor number and tunable thresholds. *Science 273:104.*
50. Novotny, J., R. E. Bruccoleri, W. D. Carlson, M. Handshucmacher, and E. Haber. 1987. Antigenicity of myohemerythrin. *Science 238:1584.*
51. Arevalo, J. H., M. J. Taussig, and I. A. Wilson. 1993. Molecular basis of cross-reactivity and the limits of antibody-antigen complementarity. *Nature 365:859.*
52. Regenmortel, M. H. V. 1995. Transcending the structuralist paradigm in immunology: affinity and biological activity rather than purely structural considerations should guide the design of synthetic peptide epitopes. *Biochem. Pept. Prot. Nucleic Acids 1:109.*
53. Wishart, D. S., and B. D. Sykes. 1994. Chemical shifts as a tool for structure determination. *Methods Enzymol. 239:363.*
54. Kabat, E. A., T. T. Wu, H. M. Perry, K. S. Gottesman, and C. Foeller. 1991. *Sequences of Proteins of Immunological Interest*, 5th Ed. U.S. Department of Health and Human Services, National Institutes of Health, Bethesda, MD.